Free Independence and the Noncrossing Partition Lattice in Dual-Unitary Quantum Circuits

Hyaline Chen

April 2025

Abstract

In this paper, we demonstrate the approach to free independence of operators in dual-unitary circuits at late times analytically. We utilizes a replica trick based on the lattice of noncrossing partitions for dual-unitary circuits which my co-author and I developed which could potentially be useful in other calculations such as for entanglement entropy. This writing is based on my work with Jonah-Kudler Flam in [1].

1 Introduction

In a quantum many-body system, spacelike separated observables, such as equal time Pauli operators, commute with each other:

$$[\sigma_\alpha(x,t), \sigma_\gamma(y,t)] = 0, \quad \alpha, \gamma \in \{x, y, z\}. \tag{1}$$

However, once they become in causal contact, their commutator grows

$$[\sigma_\alpha(x,0), \sigma_\gamma(y,t)] = O(1). \tag{2}$$

The thermal expectation value of the nontrivial piece of the square of this commutator is the so-called out-of-time-ordered correlator (OTOC)

$$C^{(2)}(x,y,t) := \langle \sigma_\alpha(x,0)\sigma_\gamma(y,t)\sigma_\alpha(x,0)\sigma_\gamma(y,t)\rangle, \tag{3}$$

Since we expect the commutator to grow, and since it is equal to a constant minus the OTOC, we expect the OTOC to decay in the long term. The OTOC is the overlap between states $AB_t|\beta\rangle$ and the one with operation reversed $B_tA|\beta\rangle$, which can be understood as a measurement of quantum butterfly effect since it calculates the overlap between the end states if we apply A before or after time evolution. This is why OTOC has been a popular diagnostic of quantum chaos in many-body systems.

However, the two-point OTOC is far from the entire story, as pointed out in [2] and [3], the OTOC could give false positives where the system is not chaotic but the OTOC decays anyway. This could be fixed by looking at the decay of all the higher point k-OTOCs, which we define as:

$$C^{(k)}(x,y,t) := \langle (\sigma_\alpha(x,0)\sigma_\gamma(y,t))^k\rangle \to 0. \tag{4}$$

which eliminates the previously stated problem. This condition of chaos can actually be rephrased using the language of free probability. Free probability is a generalization of the usual probability theory to non-commutative random variables, as developed by Dan Voiculescu around 1986 in order to attack the free group factors isomorphism problem. The higher OTOC diagnostic 4 is equivalent to the condition of free independence as defined by Voiculescu:

Given a state φ, which is a linear functional on an algebra of operators, two algebra elements a and b are *freely independent* if

$$\varphi(f_1(a)g_1(b)f_2(a)g_2(b)\dots f_n(a)g_n(b)) = 0, \quad \forall n \tag{5}$$

whenever $\varphi(f_i(a)) = \varphi(g_i(b)) = 0$, where f_i and g_i are polynomials of the operators. For thermal expectation values of Pauli operators (which are traceless), this is equivalent to (4).

At early times in the system spacelike operators usually have *tensor independence* where

$$\varphi(f_1(a)g_1(b)f_2(a)g_2(b)\dots f_n(a)g_n(b)) = \varphi(f_1(a)f_2(a)\dots f_n(a)) \times \varphi(g_1(b)g_2(b)\dots g_n(b)). \tag{6}$$

which is the usual notion of independence in ordinary probability theory. Therefore, we rephrase the investigation of thermalization of quantum systems as a study of the approach from tensor independence to free independence of originally spacelike-separated operators.

The approach to free independence can be studied numerically just by numerically evolving the operators and computing the $k - OTOCs$ directly. Analytically, it is well known mathematically that large random matrices become asymptotically free with respect to each other as the size N grows [4]. Recently, free independence for operators at late times have also been proved analytically for nonlocal systems like systems evolved by a random Wigner matrix in [5], and for some one-dimensional systems including the quantum cat map, and three paradigmatic large-N models, including the Sachdev Ye-Kitaev model in [3]. We show analytically that traceless operators in dual-unitary quantum circuits also approach asymptotical freedom, which provides new examples with which one can study analytically the late-time approach to free independence in physical, local systems without disorder and the large N limit, and which one can see building in a laboratory.

2 Dual unitary circuits

We consider a quantum circuits composed of unitary evolution operators, on two sites of local Hilbert space dimension q, $\mathbb{C}_q \otimes \mathbb{C}_q$. For simplicity, we take q to be a power of 2, so that we consider the generalized Pauli operators consisting of tensor products of 2×2 Pauli operators. We take the red block as the unitary evolution operator, and the blue block as its adjoint, note that both the operator and its adjoint has the orientation labelled by the small v-shape at the top right corners in their definitions. Then, the definition of unitarity and dual-unitarity can be written as (left is unitarity and right is dual unitarity)

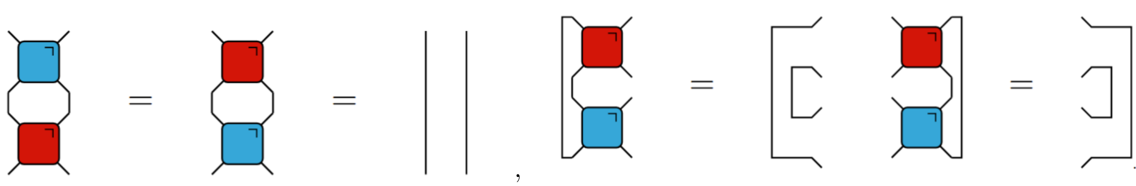
(7)

Dual-unitarity can be understood as the condition of unitarity in the spatial direction, adding extra symmetries to the problem. This condition is obeyed by a large class of physical systems ranging from ranging from maximally chaotic to the kicked Ising model at both integrable and nonintegrable points [6]. These conditions allow simplifications useful for the computation of observables.

For example, in [6] it was shown that the two point functions

$$\langle \sigma_\alpha(0,0)\sigma_\gamma(x,t)\rangle = \delta_{x,t} f_{\alpha\gamma}(t), \tag{8}$$

can be written as a product of quantum channels:

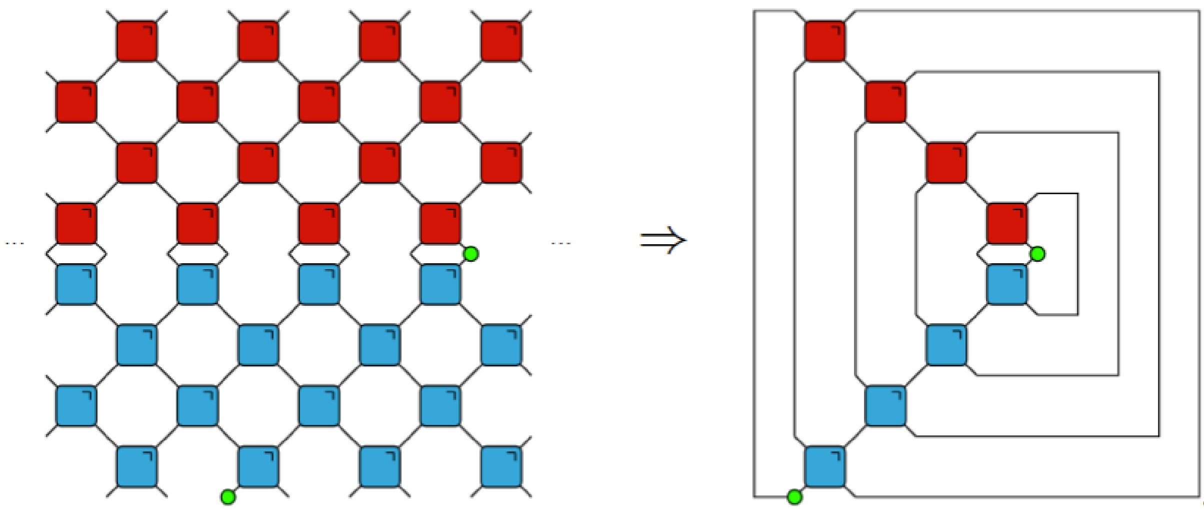

(9)

Where if we define channels as

$$\mathcal{M}_+(\sigma) = \mathrm{Tr}_1\left(U(\sigma \otimes \mathbb{1})U^\dagger\right), \quad \mathcal{M}_-(\sigma) = \mathrm{Tr}_2\left(U^\dagger(\mathbb{1} \otimes \sigma)U\right). \tag{10}$$

where graphically:

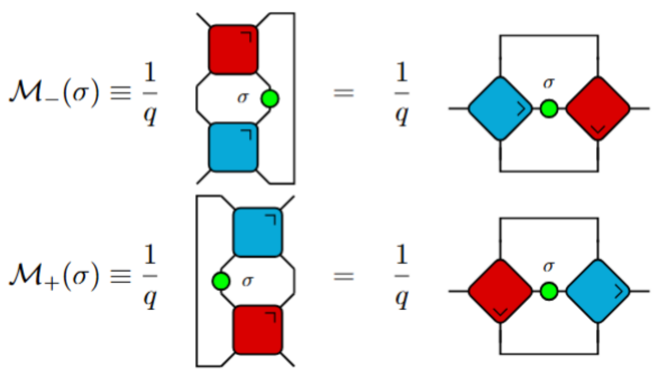

(11)

The two-point function reduces to (Note that the subscripts on the trace denote that these are partial traces over the first and second tensor factors respectively):

$$f_{\alpha\gamma}(t) = \frac{1}{q}\mathrm{Tr}\left(\sigma_\gamma \mathcal{M}_-^t(\sigma_\alpha)\right) = \frac{1}{q}\mathrm{Tr}\left(\sigma_\alpha \mathcal{M}_+^t(\sigma_\gamma)\right), \tag{12}$$

We carry out similar calculations for higher point OTOCs.

We have that the general OTOC is equal to (the different colors of Pauli operators represent the different parity of the spatial location of the two operators):

$$C_{\alpha\gamma}^{(k)}(x,t) \propto$$

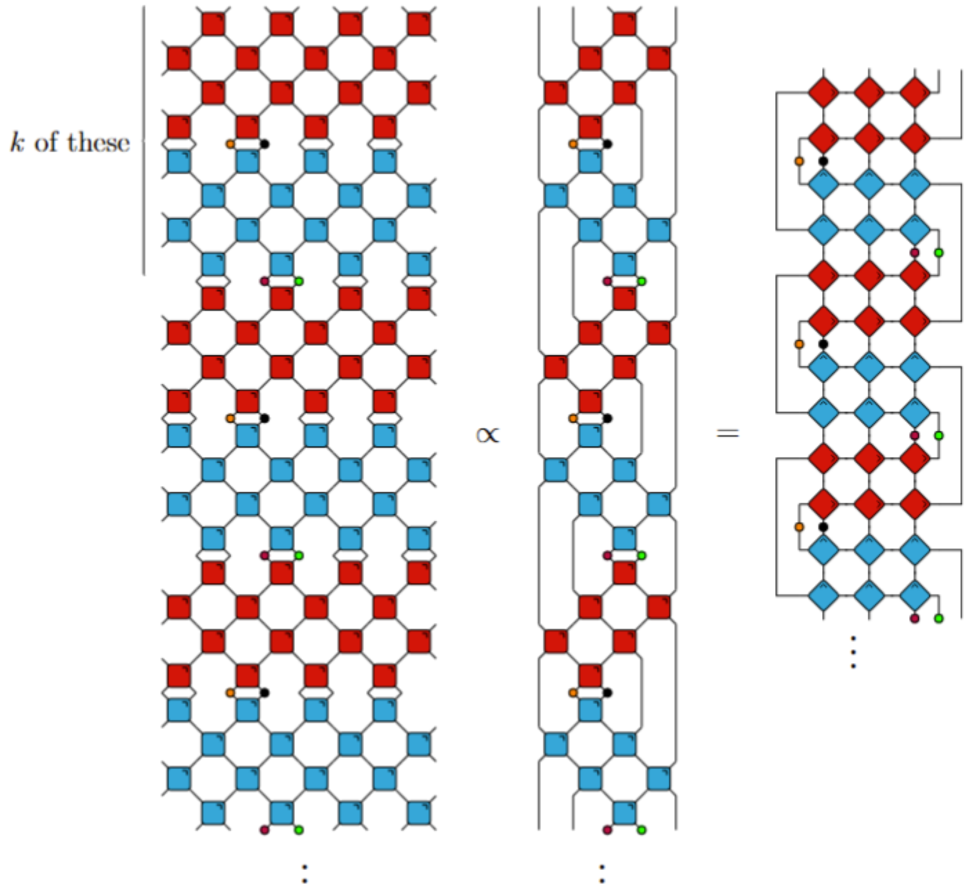

(13)

which can be written as a product of general replica transfer matrices:

$$T_n^{(1)} = \frac{1}{q} \times$$

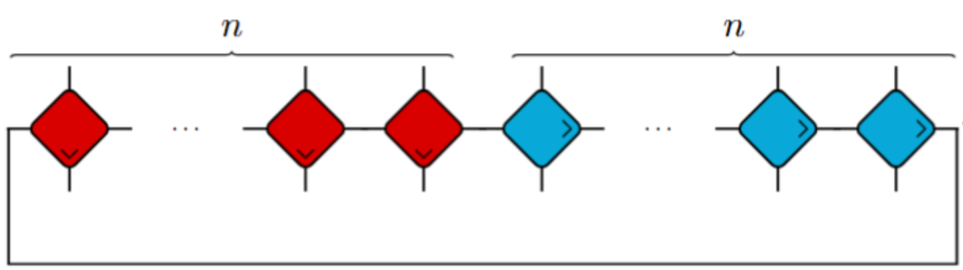

(14)

$$T_n^{(k)} = \frac{1}{q} \times$$

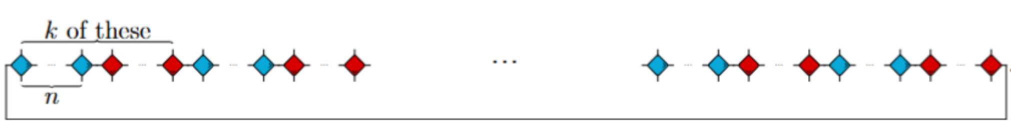

(15)

with boundary conditions

$$\langle L_1^{(k)}(\sigma_\alpha)| \equiv \frac{1}{q^{n/2}}$$
$$\langle L_2^{(k)}(\sigma_\alpha)| \equiv \frac{1}{q^{n/2+1}}$$
$$|R_1^{(k)}(\sigma_\gamma)\rangle \equiv \frac{1}{q^{n/2}}$$
$$|R_2^{(k)}(\sigma_\gamma)\rangle \equiv \frac{1}{q^{n/2+1}}$$

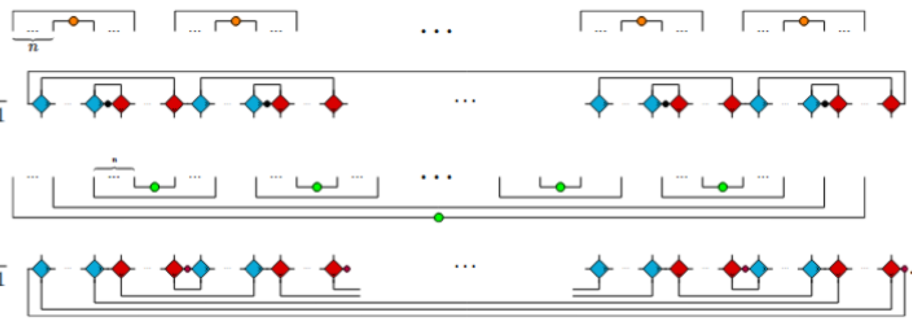

(16)

giving four possible OTOCs depending on the parity of the spatial location of the two operators:

$$\begin{aligned} C_{\alpha\gamma}^{(k),(11)}(x,t) &= \langle L_1^{(k)}(\sigma_\alpha)| \, (T_n^{(k)})^m \, |R_1^{(k)}(\sigma_\gamma)\rangle \\ C_{\alpha\gamma}^{(k),(21)}(x,t) &= \langle L_2^{(k)}(\sigma_\alpha)| \, (T_n^{(k)})^m \, |R_1^{(k)}(\sigma_\gamma)\rangle \\ C_{\alpha\gamma}^{(k),(12)}(x,t) &= \langle L_1^{(k)}(\sigma_\alpha)| \, (T_n^{(k)})^m \, |R_2^{(k)}(\sigma_\gamma)\rangle \\ C_{\alpha\gamma}^{(k),(22)}(x,t) &= \langle L_2^{(k)}(\sigma_\alpha)| \, (T_n^{(k)})^m \, |R_2^{(k)}(\sigma_\gamma)\rangle \end{aligned} \quad (17)$$

where $m = (x + t + c_m)/2$ with $c_m \in \{0, 1, 2\}$ depending on parity. The boundary conditions also depend on parity. When the orange (green) dot, denoting σ_α (σ_γ) on the left (right), is nontrivial but the black (purple) dot is trivial, we write a subscript 1 for the boundary condition. The opposite configuration is given by the subscript 2.

3 Eigenstates of the dual-unitary general k-transfer matrices

Next, we consider the large m limit, where a classification of maximal eigenvalue eigenstates of the transfer matrices will be useful. Since the transfer matrices of dual unitary circuits are contracting they have eigenvalues of modulus less or equal to 1. [6]

We observe that the eigenstates of the general k transfer matrix can be classified using the noncrossing partition lattice. This is because, using the same assumptions as in [6] of limiting ourselves to maximally chaotic systems where the only unit eigenvalue eigenstates are those necessary ones coming from dual unitary contractions, we must contract neighboring red and blue operators until all operators are annihilated in order to construct a relevant eigenstates. (The remaining loop after contractions contributes a factor of q, cancelling the $1/q$ in the transfer matrix.)

We introduce a shorthand for counting the relevant eigenstates. We remove the legs of the unitaries and replace the boxes by dots as shown below.

Using this, it is evident that each eigenstate have noncrossing contractions between red and blue dots, one for every dot. The noncrossing condition comes from the requirement that we can only eliminate red and blue blocks when they are next to each other.

In total there would be $2kn$ dots. If we go from the outmost dots in each block of 2n operators, we get n sets of contractions between 2k dots at the same depth. The outmost dots graphically is:

(18)

The contractions between these 2k dots can be written as a permutation, if we label each block with a number, and consider the number at the other end of the connection of the left point as where the original number of the block is permutated to. For example,

(19)

is the permutation which ends 1 to 2 and 2 to 1, (1,2). Each layer is then labelled by a permutation in S_k of k objects.

Not all permutations in S_k are allowed. For example,

(20)

has crossings. So we must restrict to the noncrossing permutations, NC_k, such as

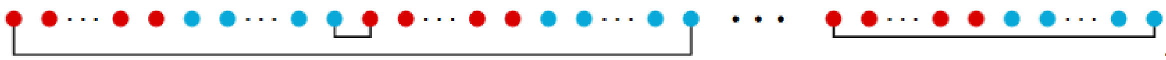

(21)

If we go in layer by layer:

(22)

We see that each layer is labelled by an element of NC_k, such that the outmost layer places restrictions on the inner layers because we don't want crossings between the deeper layers with layers outside of it. This restrcition can precisely be formulated in terms of the inclusion order on permutations.

We thus enumerate the relevant eigenstates by n-chains in the lattice of noncrossing partitions NC_k

$$|\tau_1 \geq \cdots \geq \tau_n\rangle \,. \tag{23}$$

The total number of eigenstates is given by the Fuss-Catalan numbers. We check that this formula recover the previous results in [6].

In order to solve analytically solve for $\lim_{m\to\infty}\left(T_n^{(k)}\right)^m$, we need to orthonormalize the eigenvectors. This is challenging to achieve via a Graham-Schmidt procedure in generality, because there is not a canonical ordering of n-chains. For convenience, we now take the large-q limit.

It is clear from the general result (obtainable by drawing out the contractions), where $C(\cdot)$ is the function that counts the number of cycles in the permutation, which is linearly related to the rank function:

$$\langle\tilde{\tau}_1 \geq \cdots \geq \tilde{\tau}_n|\,\tau_1 \geq \cdots \geq \tau_n\rangle = q^{\sum_i C(\tilde{\tau}_i\tau_i^{-1})}. \tag{24}$$

that in this limit, the eigenstates become asymptotically orthogonal. Normalizing this orthonormal basis gives

$$\frac{1}{q^{\frac{kn}{2}}}\,|\tau_1 \geq \cdots \geq \tau_n\rangle\,, \quad \tau_i \in NC_k \tag{25}$$

and

$$\lim_{m\to\infty}\left(T_n^{(k)}\right)^m = \frac{1}{q^{kn}}\sum_{n-chains}|\tau_1 \geq \cdots \geq \tau_n\rangle\,\langle\tau_1 \geq \cdots \geq \tau_n|\,. \tag{26}$$

4 The approach to free independence

The simplest setup is

$$\text{case I: } C_{\alpha\gamma}(x,t) = \langle L_1^{(k)}(\sigma_\alpha)| \, (T_n^{(k)})^m \, |R_1^{(k)}(\sigma_\gamma)\rangle$$

The second possibility is

$$C_{\alpha\gamma}(x,t) = \langle L_2^{(k)}(\sigma_\alpha)| \, (T_n^{(k)})^m \, |R_1^{(k)}(\sigma_\gamma)\rangle$$

which is the same as

$$C_{\alpha\gamma}(x,t) = \langle L_1^{(k)}(\sigma_\alpha)| \, (T_n^{(k)})^m \, |R_2^{(k)}(\sigma_\gamma)\rangle$$

up a rotated redefinition of U and $U^\dagger$ [1]. These are thus collectively treated as the Case II.

The third case with

$$\text{case III: } \langle L_2^{(k)}(\sigma_\alpha)| \, (T_n^{(k)})^m \, |R_2^{(k)}(\sigma_\gamma)\rangle$$

is the most difficult.

We examine these cases separately.

4.0.1 Case I

We start with the simplest set-up with $\langle L_1^{(k)}(\sigma_\alpha)| \, (T_n^{(k)})^m \, |R_1^{(k)}(\sigma_\gamma)\rangle$. Consider τ_n. In order for the projection to be non-zero on the left boundary, this must be a noncrossing permutation with only even length cycles, a set we denote NC_e. Even length cycles are necessary to form a product of an even number of Pauli matrices, which is the identity operator and hence has trace q. The product of an odd number of Pauli operators is traceless. Thus,

$$\langle L_1^{(k)}(\sigma_\alpha)| \sum_{n-chains \in NC} |\tau_1 \geq \cdots \geq \tau_n\rangle \langle \tau_1 \geq \cdots \geq \tau_n| = q^{\sum_i C(\tau_i)} \sum_{n-chains \in NC_e} \langle \tau_1 \geq \cdots \geq \tau_n| \,. \tag{27}$$

All permutations consisting of only even length cycles must include at least two cycles involving nearest neighbors. This has a significant effect because, all vectors of this type are orthogonal to $|R_1^{(k)}(\sigma_\gamma)\rangle$ as the inner product is proportional to the trace of σ_γ. Therefore, all OTOCs of this parity are trivial at large m.

4.0.2 Case II

We now look at the second case, $\langle L_1^{(k)}(\sigma_\alpha)| \, (T_n^{(k)})^m \, |R_2^{(k)}(\sigma_\gamma)\rangle$. The left boundary condition again requires that there be only even cycles in τ_n. It is evident that from 27, at large q, the permutations consisting of $k/2$ two-cycles dominate the projector when contracted with the left boundary. This fixes all τ_i to be the same. Using the Kreweras' formula for the number of noncrossing partitions of $[k]$ with partition structure $(1^{m_1} 2^{m_2} \ldots k^{m_k})$

$$\# NC_k(1^{m_1} 2^{m_2} \ldots k^{m_k}) = \frac{k!}{(k+1-\sum_i m_i)! \prod_i m_i!}. \tag{28}$$

we get that there are

$$\frac{k!}{(k/2+1)!(k/2)!} = C_{k/2} \tag{29}$$

of these, where C_i is the i^{th} Catalan number.

It is instructive to treat the $k=4$ case example explicitly. There are two elements in NC_4 with only two-cycles, $[1,2][3,4]$ and $[1,4][2,3]$. These give equal contributions because they are related by cyclicity.

Therefore, we only need to consider the $\tau_n = [1,2][3,4] = \tau_i$ term, which is proportional to

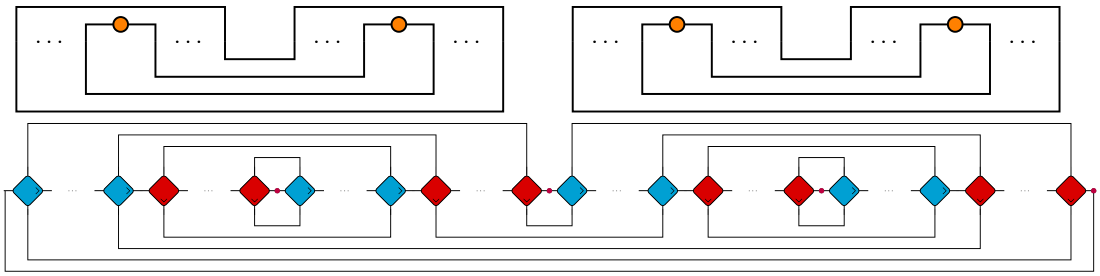

$$\propto \mathcal{N}_1^n(\sigma_\gamma)_{ab}\,\mathcal{N}_2^n(\sigma_\gamma \otimes \sigma_\gamma)_{ab,cd}\,\mathcal{N}_1^n(\sigma_\gamma)_{dc} \tag{30}$$

where the sums over repeated indices is implied. Here, we define quantum channels generalizing $\mathcal{N}_1 \equiv \mathcal{M}_+$

$$\tilde{\mathcal{N}}_m(\sigma_1 \otimes \sigma_2 \otimes \cdots \otimes \sigma_m) \equiv \frac{1}{q}$$

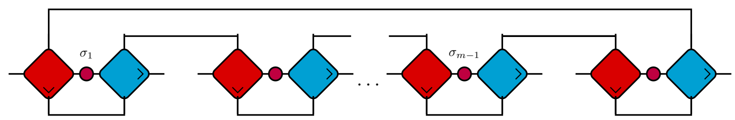

$$= \frac{1}{q}$$

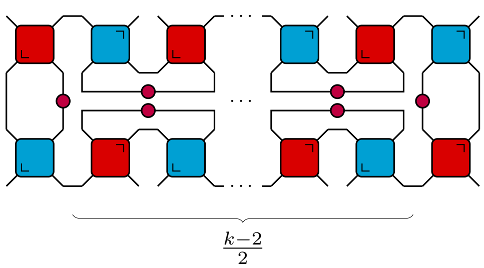

$$=$$

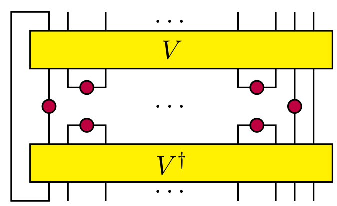

, (31)

$$= \mathcal{N}_m(\sigma_\gamma \otimes \mathcal{P}_{\sigma_\gamma}^{\otimes \frac{m-2}{2}} \otimes \sigma_\gamma)$$

where $\mathcal{P}_{\sigma_\gamma} \equiv |\sigma_\gamma\rangle\langle\sigma_\gamma|$ and $|\mathcal{O}\rangle$ is the state obtained by viewing at the operator $\mathcal{O}$ as a vector on $\mathbb{C}^q \otimes \mathbb{C}^q$, the so-called Choi–Jamiolkowski isomorphism [7, 8]. We have furthermore defined V as

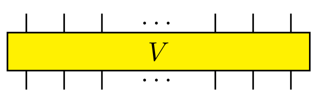

$$\equiv$$

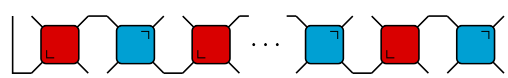

(32)

The unitarity of V ($VV^\dagger = V^\dagger V = \mathbb{1}$) follows from applying the unitarity and dual unitarity conditions of U m times. $\mathcal{N}_m$ can then be seen to be a unital quantum channels because it is the composition of a unitary and a partial trace.

From the $k = 4$ example, we see that we will need the generalized channels in the expressions of the higher k OTOCs. In fact, these are the only components we will need. The argument proceeds by representing the overall trace of the right boundary condition as a circle, which is the natural choice given the symmetry. Blue and red segments represents the U and $U^\dagger$ operators. The purple dots denote the operators on the right boundary condition (σ_γ) and orange dots denote the "dual lattice" points where the corresponding operators would be on the left boundary condition (σ_α). We can then represent the $[1,2][3,4]$ permutation in (30) as the diagram

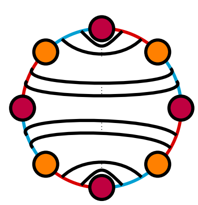

(33)

There are n lines connecting red and blue segments (the "…" between the solid lines represents $n-2$ hidden lines), representing the eigenvector of the transfer matrix which contracts with the right boundary condition. Other contractions at arbitrary k can be represented similarly.

Viewing these as permutations τ_i on Pauli operators on the left boundary condition amounts to joining the two lines adjacent to an orange dot across the orange dot, giving the graphical representation of τ_n. This is repeated $n-1$ more times to get τ_{n-1} through τ_1. In the above example, $\tau_i = [1,2][3,4]$ corresponding to the two sets of loops in the diagram

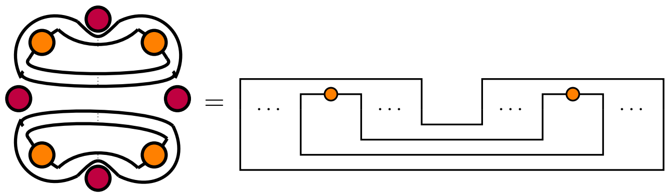

(34)

On the other hand, to see the action of quantum channels on σ_γ on the right, we note that the right boundary condition connects the lines adjacent to the purple dots with "rainbows" on the outside of the purple dots, which gives the graphical representation of the Kreweras complements of τ_1 through τ_n.

Kreweras complement, $K(\pi)$, of a partition, is the largest element of NC_k such that, when interlacing the set $[k]$ with itself, $\pi \cup K(\pi)$ remains noncrossing. Graphically, we have that if $\pi = [1,2][3,4]$, then $K(\pi) = [1][2,4][3]$:

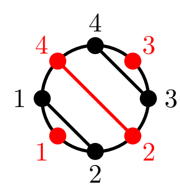

(35)

The Kreweras complement arises here because we are looking at the action of the contraction lines of a permutation as a permutation on the dual lattice points, which is the maximal complement permutation. In the $[1,2][3,4]$ example above, we have that $K([1,2][3,4]) = [1][2,4][3]$. This corresponds to $\mathcal{N}_2^n$ composed with two $\mathcal{N}_1^n$, which are given by the three sets of black loops in the diagram. These are composed as $\langle \mathcal{N}_1^n(\sigma_\gamma) | \mathcal{N}_2^n(\sigma_\gamma \otimes \sigma_\gamma) | \mathcal{N}_1^n(\sigma_\gamma) \rangle$ according to the placement of the cycles

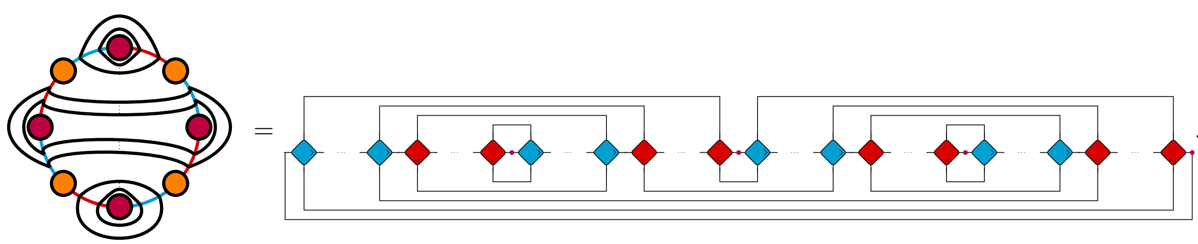

(36)

The large q limit ensures that for this second case of boundary conditions, only two-cycles contribute (so that all τ_i are identical permutations). This means we can look at all the n lines as one, and so every quantum channel that appears will appear n times

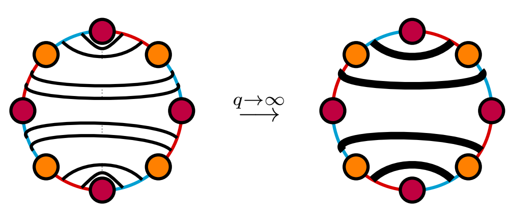

(37)

We see that the action of the contraction of eigenvectors $|\tau_1 \geq \cdots \geq \tau_n\rangle$ on the Pauli inputs $\otimes^k \sigma_\gamma$ can be expressed in terms of quantum channels of the form $\mathcal{N}_m^n$, with m taking values in the cycle lengths in $K(\tau_i)$. These $\mathcal{N}_m^n$ channels are finally contracted according to the placements of cycles in the complement of the permutation to give a contribution to the OTOC. Because of the identity $|\tau| + |K(\tau)| = k + 1$, we have that $|\tau| = k/2$ so that there are $|K(\tau)| = k/2 + 1$ many quantum channels. The maximal size of m is $k/2$, so OTOCs to the power of k are determined by the eigenvalues of $\mathcal{N}_1, \ldots, \mathcal{N}_{k/2}$

$$\begin{aligned} C_{\alpha\gamma}^{(k),(12)}(x,t) &= \frac{1}{q^{kn}} \sum_{\tau_i \in NC_k} \langle L_\alpha^1 | \tau_1 \geq \cdots \geq \tau_n \rangle \langle \tau_1 \geq \cdots \geq \tau_n | R_\beta^2 \rangle \\ &= \frac{1}{q} \sum_{\text{2-cycles } \tau \in NC_k} (\text{contractions of } \{\mathcal{N}_m^n(\sigma_\gamma \otimes \mathcal{P}_{\sigma_\gamma}^{\otimes \frac{m-2}{2}} \otimes \sigma_\gamma)\}_{\text{m cycle length of } K(\tau)}) \end{aligned} . \tag{38}$$

As n becomes large, we have

$$C_{\alpha\gamma}^{(k),(12)}(x,t) = \frac{1}{q} \sum_{\text{2-cycles } \tau \in NC_k} \prod_{m \in cycles K(\tau)} \lambda_m^n (\text{contractions of } \{\mathcal{N}_m\}) \langle \sigma_\gamma \otimes \mathcal{P}_{\sigma_\gamma}^{\otimes \frac{m-2}{2}} \otimes \sigma_\gamma | \mathcal{O}_m \rangle, \tag{39}$$

where λ_m is the maximal nontrivial eigenvalue of $\mathcal{N}_m$ with corresponding eigenoperator $\mathcal{O}_m$. From (29) we know that there are $C_{k/2}$ permutations in the sum. Crucially, the number of terms in the sum is independent of n and $m \leq k$ for a fixed k. Therefore, if each term exponentially decays with n, then the entire OTOC decays exponentially. The operator $\sigma_\gamma \otimes \mathcal{P}_{\sigma_\gamma}^{\otimes \frac{m-2}{2}} \otimes \sigma_\gamma$ is traceless, so it has no support on the identity operator whose eigenvalue was one. We expect that, generically, there are no other eigenoperators with eigenvalue one, i.e. $\lambda_m < 1$. Hence, as n becomes large, the OTOC exponentially decays with time. With knowledge of the precise unitary, λ_m may be explicitly evaluated.

4.0.3 Case III

The third case of boundary conditions is

$$\langle L_2^{(k)}(\sigma_\alpha)| (T_n^{(k)})^m |R_2^{(k)}(\sigma_\gamma)\rangle . \tag{40}$$

The left boundary condition amounts to connecting lines symmetric with respect to the green points with rainbows of n lines, and the right boundary condition amounts as before to connecting lines around the black points. Each contraction with $|\tau_1 \geq \cdots \geq \tau_n\rangle$ has the product of $\{\mathcal{N}_m\}_m$ with m corresponding to cycles in τ_i (composed from τ_n to τ_1 starting from $\otimes^k \sigma_\gamma$) and the complements of τ_i (composed from τ_1 to τ_n). Not all τ_n needs to be the same because there are no constraints for them to be only composed of two cycles

$$C_{\alpha\gamma}^{(k),(22)}(x,t) \sim \sum_{\substack{\tau_i \in NC_k \\ \tau_1 \geq \cdots \geq \tau_n}} (\text{contractions of } ((\bigotimes_{\substack{m_n \in \\ |cycles \\ K(\tau_n)|}} \mathcal{N}_{m_n}) \circ \cdots \circ (\bigotimes_{\substack{m_1 \in \\ |cycles \\ K(\tau_1)|}} \mathcal{N}_{m_1}(\sigma_\gamma \otimes \mathcal{P}_{\sigma_\gamma}^{\otimes \frac{m_1-2}{2}} \otimes \sigma_\gamma)))). \tag{41}$$

Where we are omitting some complicated combinations of SWAP and transpose operators between the compositions of each layer for the convenience of notation, but these do not change the fact that each layer is a channel nor introduce new unit eigenvectors, so do not alter the arguments.

The difficulty comes from the fact that the sum over n-chains have a number of terms proportional to $n!$, and also that the number of terms in each term in the sum is proportional to q^n. Therefore, there is no clean upper bound available. We would find it surprising if this OTOC did not exponentially decay, even though we expect a conclusive answer would require a precise specification of the unitary operators involved, given that for $x - 1$ and $x + 1$ the OTOC decays exponentially and we would expect the OTOC to be a well-behaved function of x. Furthermore, the numerical results produce exponential decay without assuming any particular parity condition, suggesting that this behaviour is generic. Numerical work as presented in [1] supports generic exponential decay behaviors for all cases of boundary conditions.

5 Conclusion and Discussions

In this paper we achieved three main goals:

Firstly, we demonstrate a connection between dual-unitary quantum circuits and free independence: We show that the operators in dual-unitary circuits at late times exhibit free independence from noncommutative probability theory. This provides fresh perspectives on how information propagates and scrambles in quantum systems and offers new tools for analyzing circuit dynamics in quantum chaotic systems, connecting the literature on free probability and thermalization.

Next, we uncover the role of the noncrossing partition lattice and develop a replica trick for dual unitary circuits: We leverage novel tools of the noncrossing partition lattice to elucidate the structure underlying dual-unitary dynamics, thus developing a replica trick for these systems. These results provide new analytic tools to investigate chaotic quantum dynamics and entanglement growth in quantum circuits and sheds light on the underlying mathematical structures in these systems.

Finally, our work is important because we prove exact results on entanglement dynamics and correlations: by writing all higher point OTOCs in terms of a general class of quantum channels, we analytically prove the exponential decay of all OTOCs in these systems, generalizing previous works in the dual-unitary literature proving only the decay of four point functions. This provides new exact results on their operator algebra structures, and offers insights into the dynamics in quantum chaotic systems. Numerical results confirm this behavior even for small onsite dimensions and finite size systems.

A few points are interesting for further discussions.

Deep thermalization is a recent topic in the literature discussing aspects of thermalization alternative to the OTOC in the context of projected ensembles as the indistinguishability of the ensemble to k-designs. It would be interesting to discuss the relationship between these different discussions of diagnostics of chaos and thermalization.

The concept of noncrossing partitions appear twice in this work separately, first of all in the moment-cumulant formula for freely independent variables, and secondly in the classification of eigenstates in dual-unitary circuits. It would be interesting to explore if there is any connections between the two.

Furthermore, the replica trick developed in this context could be useful in other calculations, such as for entanglement entropy; further investigations of applications are interesting.

References

[1] H. J. Chen, J. Kudler-Flam, Free independence and the noncrossing partition lattice in dual-unitary quantum circuits, Phys. Rev. B 111 (2025) 014311. doi:10.1103/PhysRevB.111.014311.
URL https://link.aps.org/doi/10.1103/PhysRevB.111.014311

[2] D. A. Trunin, Quantum chaos without false positives, Phys. Rev. D 108 (2023) L101703. doi:10.1103/PhysRevD.108.L101703.
URL https://link.aps.org/doi/10.1103/PhysRevD.108.L101703

[3] D. A. Trunin, Refined quantum lyapunov exponents from replica out-of-time-order correlators, Phys. Rev. D 108 (2023) 105023. doi:10.1103/PhysRevD.108.105023.
URL https://link.aps.org/doi/10.1103/PhysRevD.108.105023

[4] J. A. Mingo, R. Speicher, Free probability and random matrices, Vol. 35, Springer, 2017.

[5] G. Cipolloni, L. Erdős, D. Schröder, Thermalisation for wigner matrices, Journal of Functional Analysis 282 (8) (2022) 109394. doi:https://doi.org/10.1016/j.jfa.2022.109394.
URL https://www.sciencedirect.com/science/article/pii/S0022123622000143

[6] P. W. Claeys, A. Lamacraft, Maximum velocity quantum circuits, Physical Review Research 2 (3) (2020) 033032. arXiv:2003.01133, doi:10.1103/PhysRevResearch.2.033032.

[7] M.-D. Choi, Completely positive linear maps on complex matrices, Linear algebra and its applications 10 (3) (1975) 285–290.

[8] A. Jamiołkowski, Linear transformations which preserve trace and positive semidefiniteness of operators, Reports on mathematical physics 3 (4) (1972) 275–278.